JOC The Journal of Organic Chemistry

Article

pubs.acs.org/joc

Aminolysis of Phenyl *N*-Phenylcarbamate via an Isocyanate Intermediate: Theory and Experiment

Sonia Ilieva,* Didi Nalbantova, Boriana Hadjieva, and Boris Galabov*

Department of Chemistry and Pharmacy, University of Sofia, Sofia 1164, Bulgaria

Supporting Information

ABSTRACT: A comprehensive examination of the mechanism of the uncatalyzed and base-catalyzed aminolysis of phenyl *N*-phenylcarbamate by theoretical quantum mechanical methods at M06-2X/6-311+G(2d,2p) and B3LYP-D3/6-31G(d,p) levels, combined with an IR spectroscopic study of the reaction, was carried out. Three alternative reaction channels were theoretically characterized: concerted, stepwise via a tetrahedral intermediate, and stepwise involving an isocyanate intermediate. In contrast to dominating views, the theoretical results revealed that the reaction pathway through the isocyanate intermediate (E1cB) is energetically favored. These conclusions were supported by an IR spectroscopic investigation of the interactions of phenyl *N*-phenylcarbamate with several amines possessing varying basicities and nucleophilicities: *n*-butylamine, diethylamine, triethylamine, *N*-methylpyrrolidine, and trimethylamine. The reactivity of substituted phenyl *N*-phenylcarbamates in the aminolysis reaction was rationalized using theoretical and experimental reactivity indexes: electrostatic potential at nuclei (EPN), Hirshfeld and NBO atomic charges, and Hammett constants. The obtained quantitative relationships between these property descriptors and experimental kinetic constants reported in the literature emphasize the usefulness of theoretical parameters (EPN, atomic charges) in characterizing chemical reactivity.

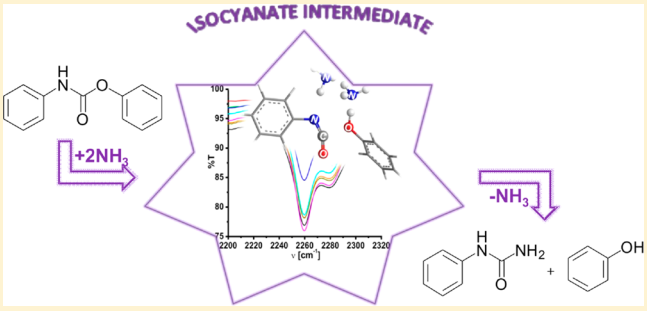

INTRODUCTION

Alternative interpretations of the mechanism of carbamate aminolysis can be found in the literature.[1−8] The carbamates possess structural similarity with esters and carbonates. Nucleophilic attack at the CO−O ester group has been discussed as a key feature in the mechanisms of aminolysis of all three classes of compounds.[2−22] Depending on the structure of the leaving group, a stepwise mechanism via a tetrahedral intermediate or concerted pathway have been proposed for the ester aminolysis.[9−22] This reaction has been the focus of numerous studies because it is the key process in the formation of peptide bonds in living organisms.[19,23] Carbamate derivatives form a major class of acetylcholinesterase (AChE) and butyrylcholinesterase (BChE) inhibitors.[21,22] The inhibitory interaction between carbamates and cholinesterases is employed as a basis for target-oriented drug design. The detailed knowledge of the mechanisms of solvolytic reactions of carbamates is of substantial interest because of their significance in research on the mechanisms of AChE and BChE inhibition.

The alkaline hydrolysis of carbamates has been intensively studied.[24] The influence of substituents and leaving group structure on the reaction mechanism has also been explored.[24d,e] Bergon and Calmon[24e] reported for the alkaline hydrolysis of methyl carbanilates that a mechanistic shift takes place depending on the nature of aromatic substituents. Electron-withdrawing groups in the *N*-aryl ring favor an addition−elimination route ($B_{AC}2$) with nucleophilic attack at the carbonyl carbon, while electron-donating aryl substituents favor an elimination−addition mechanism (E1cB) via an isocyanate intermediate. In an earlier work, Hegarthy and Frost[24d] established for a series of aryl *N*-arylcarbamates that the hydrolysis proceeds along the E1cB mechanism via isocyanate. A shift to the $B_{AC}2$ mechanism was found, however, for carbamates containing poorer leaving (alkoxy) groups. These authors also established that the reaction is base catalyzed. Thus, the literature data reveal two alternative pathways for the alkaline hydrolysis as a function of the nature of aromatic substituents and the structure of the leaving group.

On the basis of kinetic studies, the currently accepted mechanism for the aminolysis of aryl *N*-phenylcarbamates assumes an analogous stepwise pathway, involving an initial attack at the ester moiety by the amine nucleophile leading to the formation of a tetrahedral intermediate (Scheme 1).[2−8] A concerted mechanism is reported by Lee et al.[4] for the aminolysis of aryl *N*-phenylthiocarbamates. However, in an early work Menger and Glass[1] discussed two alternatives (E2 and E1cB) for the aminolysis of aryl *N*-phenylcarbamate, both involving the formation of an isocyanate intermediate in the key reaction stage. In 1986 Shawali et al.[2] reinvestigated the kinetics of aminolysis of mono- and disubstituted phenyl *N*-phenylcarbamates. The authors also conducted crossover synthetic

Received: January 30, 2013
Published: June 4, 2013

dx.doi.org/10.1021/jo4002068 | J. Org. Chem. 2013, 78, 6440−6449

Scheme 1. Possible Mechanisms for the Aminolysis of Phenyl *N*-phenylcarbamate: Concerted, Stepwise ($B_{AC}2$), and E1cB Mechanisms through Isocyanate

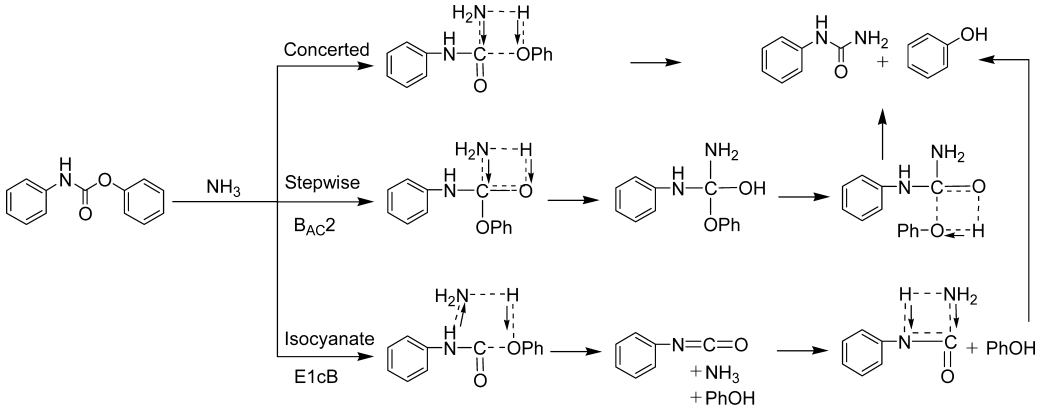

experiments and IR spectroscopic analysis of reaction mixtures to examine the possibility for a E1cB mechanism (via isocyanate) of the reaction. The experiments did not provide evidence for the formation of an isocyanate intermediate. These results led the authors to reject the possibility of a E1cB mechanism. Their results were in agreement with earlier studies of Furuya et al.[25,26] The conclusions of a later kinetic study of Lee et al.[3] were also in accord with these views on the mechanistic pathway for the aminolysis of aryl *N*-arylcarbamates. Parallel with the kinetic studies, Lee et al.[3] analyzed the 2275−2240 cm^{-1} region in the infrared spectra of reaction mixtures but did not find evidence for the formation of an isocyanate intermediate.

In the present work we apply theoretical quantum mechanical methods to model the aminolysis of phenyl *N*-phenylcarbamate for molecules in isolation (gas phase) and in the reactant amine medium. In contrast to the dominating views, our theoretical results provide strong evidence that the most favorable mechanism of the reaction is E1cB, involving the intermediary formation of phenyl isocyanate. The energy profile of the reaction along the isocyanate pathway is 7 kcal/mol lower that the alternative routes through stepwise or concerted mechanisms with nucleophile attack at the ester moiety. Our theoretical conclusions were supported by specially designed IR spectroscopic experiments on the reactions of phenyl *N*-phenylcarbamate with amines with similar basicity: *n*-butylamine, diethylamine, and triethylamine. The experiments provided strong evidence for the formation of phenyl isocyanate as an intermediate. Theoretical computations and correlations with the experimental kinetic data of Shawali et al.[2] also revealed the nature of intramolecular charge rearrangements determining the reactivity of aryl *N*-phenylcarbamates for the reaction examined.

EXPERIMENTAL SECTION

Spectroscopy Experiments. The reactions between phenyl *N*-phenylcarbamate and four amines (*n*-butylamine, diethylamine, triethylamine, *N*-methylpyrrolidine) were followed by FTIR spectroscopy. IR spectra of reaction mixtures of the reactant carbamate and excess amines (1:6) in CCl_4 were recorded for several hours at room temperature and at 76 °C (boiling temperature of CCl_4) in a 0.28 mm NaCl cell. The interaction of phenyl *N*-phenylcarbamate in CCl_4 with trimethylamine (in a 1:1 solution in tetrahydrofuran and carbon tetrachloride) was also followed by IR spectroscopy.

Computational Methods. Density functional theory computations were conducted by employing the Gaussian 09 program package.[27] The geometry parameters of the reactant complexes, intermediates, transition states, and products of the reaction studied were fully optimized in the gas phase at the DFT level with B3LYP[28] and M06-2X[29] functionals in combination with 6-31G(d,p) and 6-311+G(2d,2p)[30] basis sets. The hybrid meta exchange-correlation functional M06-2X has been systematically tested by comparing its performance to other functionals for a variety of databases and is recommended for applications involving main-group thermochemistry, kinetics, and noncovalent interactions.[29] The basis set employed in the present research is of similar quality as some of the basis sets used in assessing the performance of the M06-2X functional.[29b] The DFT-D3 dispersion corrections introduced by Grimme et al.[31,32] were applied to the energies of all B3LYP optimized structures. The attacking amine nucleophile is modeled with an ammonia molecule. Each stationary point along the reaction path was characterized as a minimum or as a first-order saddle point with one imaginary frequency (for the transition states) by frequency computations at the same level. The zero-point vibrational energies (ZPE) and Gibbs free energies for all structures were determined. All transition states were proved by applying the intrinsic reaction coordinate (IRC)[33] methodology.

Solvent effects were simulated with the self-consistent reaction field (SCRF) method based on the integral equation formalism of the polarized continuum model (IEFPCM).[34] The standard dielectric constant for the *n*-butylamine reaction medium, implemented in the Gaussian program, was employed. The catalytic effect of a second ammonia molecule was also considered. Thus, the aminolysis reaction was modeled as uncatalyzed and base-catalyzed processes. Full optimization of all structures in *n*-butylamine solution was performed.

The following reactivity indexes for the reaction center atoms were computed at the M06-2X/6-311+G(2d,2p) level: electrostatic potential at nuclei (EPN; V_N, V_H),[35,36] natural bond orbital (NBO) charges,[37] and Hirshfeld atomic charges.[38] The Hammett σ constants[39,40] were also applied in characterizing reactivity.

The electrostatic potential at a nucleus Y can be expressed as follows (in atomic units, boldface type denotes vector quantities):[36]

$$V_Y \equiv V(\mathbf{R}_Y) = \sum_{A(\neq Y)} \frac{Z_A}{|\mathbf{R}_A - \mathbf{R}_Y|} - \int \frac{\rho(\mathbf{r})}{|\mathbf{r} - \mathbf{R}_Y|}\, d\mathbf{r} \quad (1)$$

Z_A is the nuclear charge of atom A with position vector $\mathbf{R}_A$, and $\rho(\mathbf{r})$ is the electron density at point $\mathbf{r}$. Equation 1 contains a summation over all atomic nuclei, treated as positive point charges, as well as integration over the continuous distribution of the electronic charge. Unlike atomic charges, which depend strongly on their definition and additional approximations, the EPN values are rigorously defined quantum mechanical quantities. Because of the $1/\mathbf{r}$ dependence of the electrostatic potential, a greater contribution to V_Y comes from the local positive and negative charges around the respective atomic sites.

dx.doi.org/10.1021/jo4002068 | J. Org. Chem. 2013, 78, 6440−6449

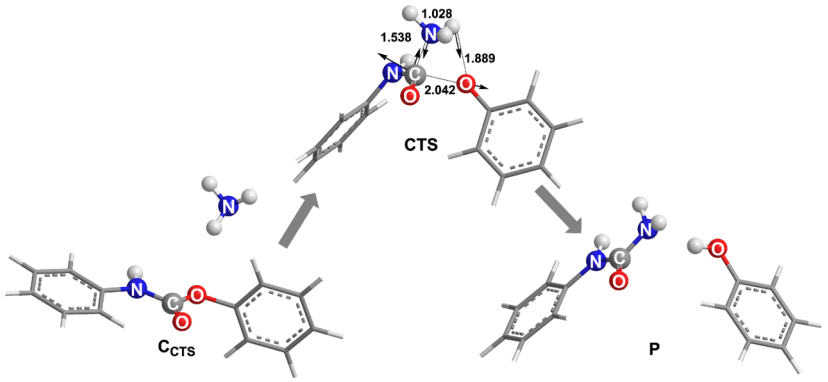

Figure 1. IEFPCM/M06-2X/6-311+G(2d,2p) optimized structures along the concerted aminolysis of phenyl *N*-phenylcarbamate.

RESULTS AND DISCUSSION

As already pointed out, different reaction channels for the aminolysis of aryl N-arylcarbamates are possible. In this work we modeled theoretically the reaction pathways along the three mechanisms discussed in the literature: concerted and addition−elimination ($B_{AC}2$) of the ester moiety as well as elimination−addition (E1cB) mechanism through an isocyanate intermediate. These three possibilities are illustrated in Scheme 1. Earlier computational results on the aminolysis of esters[17,18] showed that the concerted pathway involves an initial nucleophilic attack along the C−O ester bond, while the stepwise addition−elimination route begins with attack at the carbonyl C═O bond. In the initial stage of the elimination−addition E1cB mechanism the nucleophile deprotonates the reactant carbamate, resulting in the formation of a phenyl isocyanate intermediate.

As already mentioned, theoretical computations (full optimization and frequency calculations) of all critical structures along the three reaction pathways (Scheme 1) have been performed at two levels of theory—B3LYP-D3/6-31G(d,p) and M06-2X/6-311+G(2d,2p)—in both the gas phase and simulated *n*-butylamine solution. The obtained theoretical results are presented in detail in Tables S1−S4 of the Supporting Information. The IEFPCM/M06-2X/6-311+G-(2d,2p) results for the reaction profiles are further discussed. The two theoretical methods employed provide similar energy profiles of the studied processes.

Reaction Channels for the Aminolysis of Phenyl *N*-Phenylcarbamate. *Concerted Mechanism.* This potential reaction channel for the aminolysis of carbamates has been studied in the case of ester aminolysis.[17] As was mentioned, the mechanistic pathway involves an attack of the nucleophile along the ester C−O single bond, leading to the formation of a transition state. The optimized structure of the concerted transition state (**CTS**) in simulated *n*-butylamine medium is shown in Figure 1.

The arrows in the transition state structures indicate the normal coordinate of the imaginary frequency. The normal mode vector of the imaginary frequency involves simultaneous cleavage of the ester C−O bond and creation of the new urea C−N bond. In **CTS** the distance between the carbonyl carbon and the ester oxygen atoms is much longer (2.042 Å at IEFPCM/M06-2X/6-311+G(2d,2p)) than the respective C−O ester bond in the reactant phenyl *N*-phenylcarbamate (1.364 Å). The new C−N bond is close to formation with a length of 1.538 Å in **CTS** in comparison to 1.395 Å in the product *N*,*N*′-diphenylurea. The IRC computations in the backward direction from the concerted transition state **CTS** lead to the prereactive complex $\mathbf{C}_{CTS}$ between the reactants.

Stepwise Addition−Elimination ($B_{AC}2$) Mechanism. The stepwise addition−elimination pathway for the aminolysis of phenyl *N*-phenylcarbamate involves two main stages. Again, this potential reaction channel has been established to dominate the aminolysis of certain esters.[17] The principal transition state structures along the addition−elimination pathway of phenyl *N*-phenylcarbamate aminolysis are shown in Figure 2. The first stage of the reaction is the addition of an

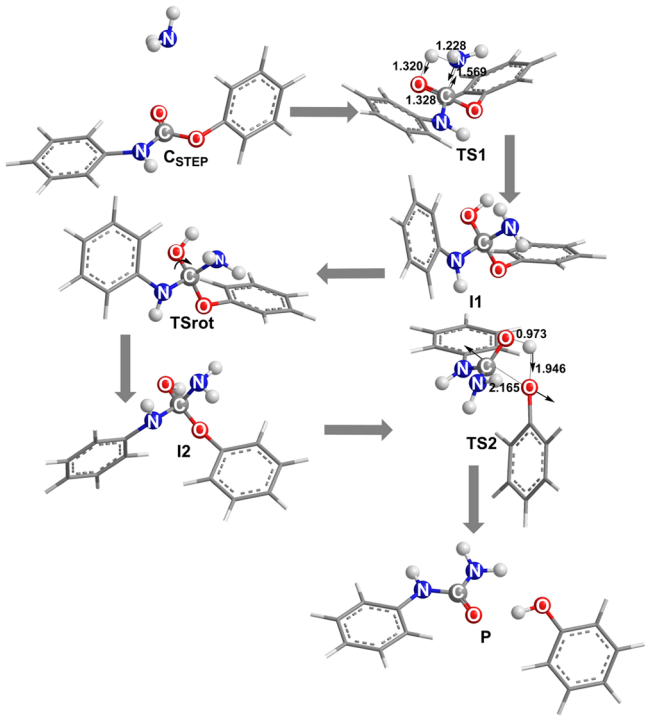

Figure 2. IEFPCM/M06-2X/6-311+G(2d,2p) optimized structures along the stepwise mechanism via a tetrahedral intermediate for the aminolysis of phenyl *N*-phenylcarbamate.

N−H bond from the nucleophile to the carbonyl double bond and formation of a tetrahedral intermediate (transition state **TS1**, free energy barrier of 54.03 kcal/mol; Table 1). The main vectors of the imaginary vibrational frequency for **TS1** are shown in Figure 2 and correspond to the C−N bond formation and a proton transfer from the nucleophile NH_3 to the carbonyl oxygen, thus maintaining the neutrality of the forming

dx.doi.org/10.1021/jo4002068 | J. Org. Chem. 2013, 78, 6440−6449

Table 1. M06-2X/6-311+G(2d,2p) Computed Relative to Reactant Energies in kcal/mol for the Transition State Structures along the *Uncatalyzed* Concerted, Stepwise ($B_{AC}2$), and Isocyanate (E1cB) Mechanisms in the Gas Phase and in Simulated *n*-Butylamine Medium

	gas phase		in *n*-butylamine	
structure	ΔE	ΔG	ΔE	ΔG
CTS	39.77	49.54	33.59	43.31
TS1	44.32	55.31	44.37	54.03
TSrot	14.11	25.68	15.84	27.25
TS2	26.97	37.86	25.75	35.58
IsoTS1	25.19	33.95	22.17	30.02
IsoTS2	32.06	40.66	33.58	43.19

tetrahedral intermediate. At the same time a change of the hybridization of the carbonyl carbon from sp^2 to sp^3 takes place. The C═O bond is extended from 1.203 Å in the reactant to 1.329 Å in **TS1**. The new C−N bond has a length of 1.569 Å in the **TS1** transition state. IRC computations from **TS1** in the forward direction lead to the tetrahedral intermediate **I1**.

In the second stage the tetrahedral intermediate converts to the products phenylurea and phenol via transition state **TS2** (free energy barrier of 35.58 kcal/mol; Table 1). Breaking of the C−O ester single bond and simultaneous restoration of the C═O bond takes place following a proton transfer between the two oxygen atoms. The process of breaking/restoring occurs after a proper space orientation of the O−H hydrogen atom through a rotation that facilitates the proton-transfer process. The rotation through **TSrot** (Figure 2) involves a free energy barrier of 27.25 kcal/mol (Table 1).

E1cB Mechanism through Isocyanate. The third theoretically modeled reaction channel for the aminolysis of phenyl *N*-phenylcarbamate is the E1cB pathway, consisting of two subsequent reactions with the intermediary formation of phenyl isocyanate, suggested first by Menger and Glass.[1] The optimized structures of the stationary points along the isocyanate pathway are shown in Figure 3. The first step of the reaction is the formation of phenyl isocyanate and phenol. The attacking NH_3 nucleophile deprotonates the carbamate nitrogen, while the C−O ester single bond breaks. A simultaneous proton transfer from the carbamate nitrogen toward the ester oxygen mediated by the nucleophile NH_3 takes place to form the phenol molecule (Figure 3). These processes are reflected in the main vectors of the imaginary vibrational frequency of the first transition state **IsoTS1** (free energy barrier of 30.02 kcal/mol; Table 1), shown in Figure 3. Thus, one of the final products of the aminolysis—phenol—is formed during this first process of the E1cB pathway.

The second step of the process involves the addition of ammonia to the nitrogen−carbon double bond of the phenyl isocyanate leading to the product phenylurea through the transition state **IsoTS2**. In this transition state the new C−N urea bond is created. The main component of the transition vector in **IsoTS2** corresponds to a proton transfer between the two nitrogen atoms (Figure 3).

The relative energies of the structures along the *concerted*, *addition−elimination stepwise,* and *isocyanate* pathways computed at M06-2X/6-311+G(2d,2p) are summarized in Table 1. It can be seen that the evaluated free energy reaction barrier in modeled *n*-butylamine medium for the isocyanate mechanism is more favorable in comparison to the concerted and addition−elimination stepwise pathways, respectively.

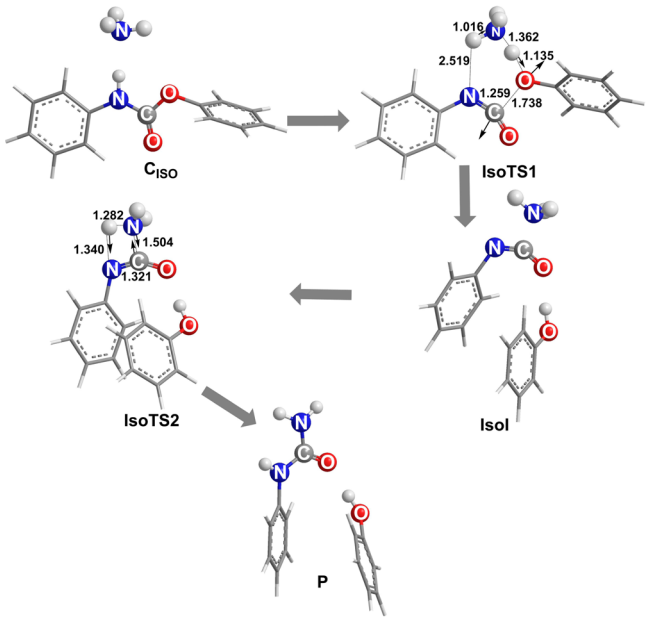

Figure 3. IEFPCM/M06-2X/6-311+G(2d,2p) optimized structures along the two-stage mechanism for the aminolysis of phenyl *N*-phenylcarbamate proceeding through formation of isocyanate in the first step.

An intriguing problem emerges comparing computed energies of the two transition states along the isocyanate path (Table 1). The transition state **IsoTS2** has higher energy with regard to **IsoTS1**. It is known, however, that isocyanates are highly reactive species. We followed experimentally the reaction between phenyl isocyanate and excess *n*-butylamine (1:3) in CCl_4 at room temperature. The interaction is very fast, and the isocyanate band (2260 cm^{-1}) cannot be registered by IR spectroscopy (Figure S1 in the Supporting Information). It is expected, therefore, that the first step of the aminolysis—formation of the phenyl isocyanate—should be the rate-determining stage. In order to resolve the discrepancy and take into account that the experimental aminolysis is carried out in the liquid phase with excess amine, we considered the general base catalysis of the process. This catalytic process is modeled by explicitly considering the participation of a second nucleophile molecule in the three reaction channels.

General Base Catalysis. Under experimental conditions the ester aminolysis reaction can take place as a catalyzed process with a catalytic role of the nucleophile amine.[10] The potential energy surfaces for the general base-catalyzed aminolysis of phenyl *N*-phenylcarbamate along the three pathways considered was searched by performing full optimization of the stationary points at the M06-2X/6-311+G(2d,2p) level of theory in the gas phase and in modeled *n*-butylamine solution (IFPCM). The estimated energies of the process via the three routes are given in Table 2 and visualized in Figure 4. Transition state structures for the concerted, stepwise addition−elimination, and isocyanate pathways of the catalyzed aminolysis of phenyl *N*-phenylcarbamate are presented in Figure 5.

The catalytic role of the second ammonia molecule mostly affects the proton-transfer processes. The catalyst facilitates the hydrogen transfer by forming proton transfer chains, thus lowering the energy barriers. This deduction is supported by the present computational results for the directions of the

dx.doi.org/10.1021/jo4002068 | J. Org. Chem. 2013, 78, 6440−6449

Table 2. M06-2X/6-311+G(2d,2p) Relative to Reactant Energies in kcal/mol for the Transition State Structures along the *Catalyzed* Concerted, Stepwise Addition–Elimination, and Isocyanate Mechanisms in the Gas Phase and in *n*-Butylamine

	gas phase		in *n*-butylamine	
structure	ΔE	ΔG	ΔE	ΔG
CTS^{CAT}	22.32	43.01	21.44	41.57
TS1^{CAT}	21.01	42.31	19.75	40.77
TS2^{CAT}	11.82	32.20	12.97	33.20
IsoTS1^{CAT}	15.07	32.87	16.49	33.85
IsoTS2^{CAT}	9.88	28.73	5.99	23.01
IsoTS2^{CAT}* [a]			−0.13	19.04

[a] **IsoTS2^{CAT}*** energies are relative to isolated PhNCO and 2NH_3.

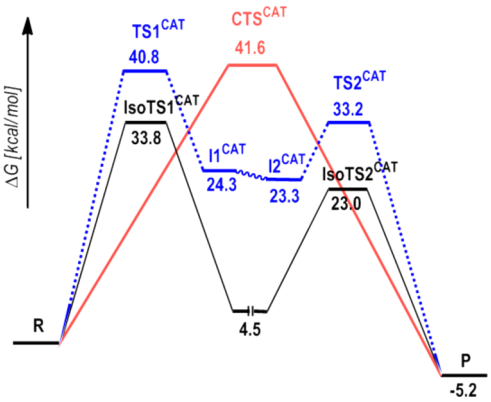

Figure 4. Energy diagram for the catalyzed aminolysis of phenyl *N*-phenylcarbamate along the concerted, addition–elimination stepwise, and isocyanate pathways from IEFPCM/M06-2X/6-311+G(2d,2p) computations.

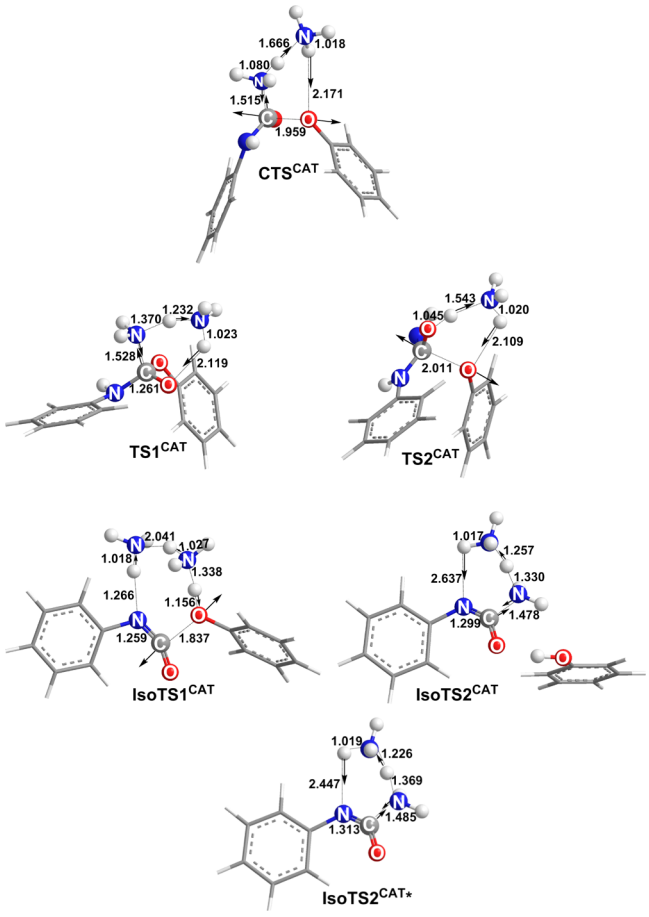

Figure 5. IEFPCM/M06-2X/6-311+G(2d,2p) optimized transition states for the concerted, stepwise ($B_{AC}2$), and isocyanate (E1cB) pathways for the catalyzed aminolysis of phenyl *N*-phenylcarbamate.

transition vectors characterizing the **CTS^{CAT}**, **TS1^{CAT}**, **TS2^{CAT}**, **IsoTS1^{CAT}**, and **IsoTS2^{CAT}** structures. The transition state **IsoTS2^{CAT}** can be realized with different hydrogen bonds between phenyl isocyanate, ammonia and phenol. The lowest energy transition state structure with a C═O···H−OPh hydrogen bond is presented in Figure 5 and is taken into account when reading energy barriers. Under the reaction conditions of excess NH_3 nucleophile in the reaction medium, the phenol product of the first reaction stage converts into phenolate. Thus, the next process can be regarded as direct addition of the nucleophile to the isocyanate via the transition state **IsoTS2^{CAT}*** (Figure 5). Again, this is a low-energy transition state (Table 2; ΔE = −0.13 kcal/mol, ΔG = 19.04 kcal/mol, calculated relative to isolated PhNCO and two NH_3 molecules) and the overall activation energy is determined by the isocyanate formation stage.

Considerable lowering of the second transition state energy for the general base-catalyzed aminolysis along the isocyanate pathway was obtained in comparison to the uncatalyzed process (Table 2). Thus, the rate-determining stage of the catalyzed process is the formation of phenyl isocyanate—the first step through **IsoTS1^{CAT}**. The obtained theoretical results (Table 2, Figure 4) reveal that the free energy barrier of the isocyanate pathway is distinctly lower (by 7–7.8 kcal/mol) than the activation barriers of the two alternative reaction channels for the aminolysis of phenyl *N*-phenylcarbamate. This conclusion is strongly supported by the kinetic experiments of Menger and Glass.[1] These authors found that the aminolysis of *p*-nitrophenyl *N*-phenylcarbamate is at least 10^4 faster than the aminolysis of *p*-nitrophenyl *N*-methyl-*N*-phenylcarbamate, where isocyanate mechanism is unfeasible since N−H is replaced by N−CH_3. The energetics of the modeled reaction pathways for the aminolysis of these two carbamates along the $B_{AC}2$ mechanism are compared in Table S5 (Supporting Information). The IEFPCM/M06-2X/6-311+G(2d,2p) calculated free energy barrier for the catalyzed aminolysis of phenyl *N*-methyl-*N*-phenylcarbamate through a stepwise $B_{AC}2$ mechanism in *n*-butylamine is 42.06 kcal/mol. The respective energy barrier for the aminolysis of phenyl *N*-phenylcarbamate is 40.77 kcal/mol (Table 2). The results reveal that the rate-controlling barriers for these processes differ by only 1.3 kcal/mol. It is, therefore, unlikely that the aminolysis of phenyl *N*-phenylcarbamate would proceed along a $B_{AC}2$ mechanism, since the reaction rates for the two processes considered would not differ substantially, in contrast to the kinetic results of Menger and Glass.[1] The estimated barrier for the reaction proceeding along the E1cB mechanism via isocyanate is distinctly lower at 33.85 kcal/mol (Table 2).

The second stage of the reaction along the E1cB mechanism may follow two alternative routes, since nucleophilic attack is possible along the C═N and C═O isocyanate bonds. These two possibilities were theoretically explored for the base-catalyzed processes in modeled *n*-butylamine medium. The results are presented in Table S6 (Supporting Information). The conversion of the phenyl isocyanate in phenylurea through

dx.doi.org/10.1021/jo4002068 | J. Org. Chem. 2013, 78, 6440–6449

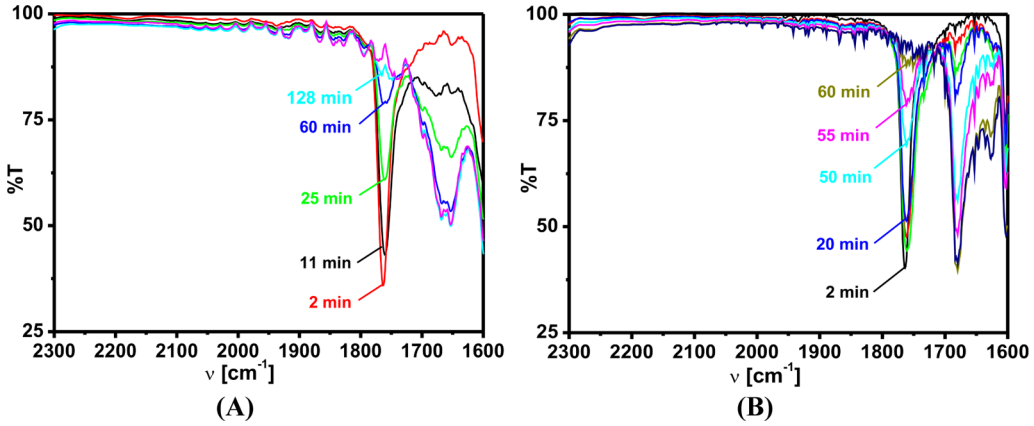

Figure 6. IR spectra of the reaction mixture of phenyl *N*-phenylcarbamate and excess *n*-butylamine (A) and diethylamine (B) in carbon tetrachloride solution taken for several hours at 76 °C (boiling temperature of CCl_4).

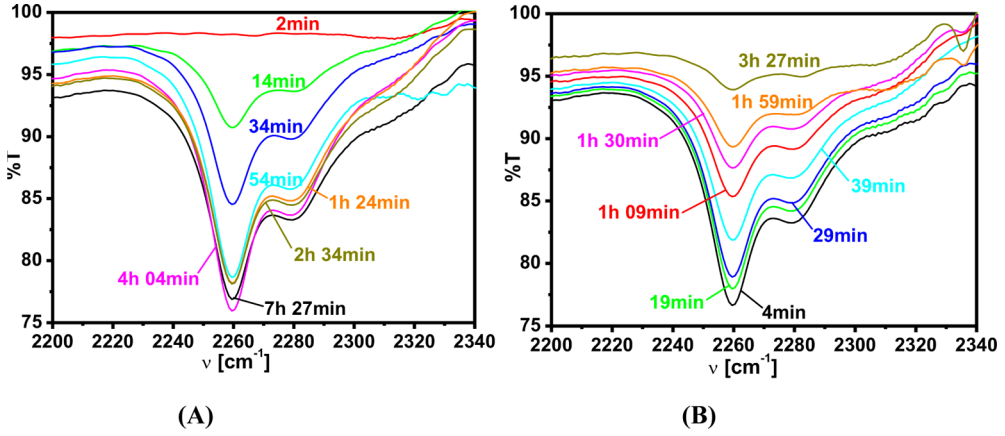

Figure 7. (A) Formation of phenyl isocyanate from phenyl *N*-phenylcarbamate and triethylamine at 76 °C in CCl_4. (B) Gradual disappearance of the N═C═O band at room temperature.

the attack of the nucleophile along the C═O isocyanate bond takes place in two steps with formation of an intermediate: the first step is the attack itself, followed by a rotation of the OH group for obtaining the proper orientation for the next proton transfer resulting in reaction products. The optimized transition state structures are given in Figure S2 (Supporting Information). The theoretical results (Table S6) showed that the nucleophilic attack along the C═N isocyanate bond is energetically favored by 2.3 kcal/mol. This conclusion is also supported by the comparative study of Muchall and coauthors,[41] who established that isocyanates hydrolyze predominantly along the C═N bond. These authors found that the modeling of two explicit nucleophile molecules is sufficient for a correct description of the process. Two explicit ammonia molecules are taken into account in our study for the base-catalyzed aminolysis.

Experiments. As already discussed, Menger and Glass[1] proposed an E1cB mechanism through isocyanate for the aminolysis of *p*-nitrophenyl *N*-phenylcarbamate with diethylamine in toluene. Shawali et al.,[2] however, excluded the presence of an isocyanate intermediate in the aminolysis of phenyl *N*-phenylcarbamate on the basis of IR spectroscopic experiments.

To verify our theoretical results and the above considerations, we conducted an IR spectroscopic study on the reaction of phenyl *N*-phenylcarbamate with *n*-butylamine (pK_a = 10.77)[42] in carbon tetrachloride medium. The analysis of the IR spectra of reaction mixtures (Figure 6A) taken for several hours at room temperature and at 76 °C (boiling temperature of CCl_4) did not reveal the formation of an isocyanate group (in the 2280−2240 cm^{-1} region), in accord with the earlier findings of Shawali et al.[2] and Lee et al.[3] Such a result is not surprising, however, in view of the high reactivity of the isocyanate in the reaction with *n*-butylamine. Therefore, the detection of a stable intermediate for this process is unlikely, as confirmed experimentally. Figure 6A shows the gradual reduction of intensity of the carbamate C═O stretching band (at 1760 cm^{-1}) and the rising intensity of the product urea C═O stretching at 1654 cm^{-1}. The reaction of phenyl *N*-phenylcarbamate with the more basic diethylamine (pK_a = 11.02)[42] proceeds in a similar way (Figure 6B). No isocyanate band in the 2280−2240 cm^{-1} spectral region is found during the process.

To analyze further the interaction between an amine and the carbamate, we conducted analogous experiments employing triethylamine as a nucleophile. Triethylamine (pK_a = 10.75)[42] has a basicity similar to that of *n*-butylamine and diethylamine. At room temperature, no interaction between the two reactants in CCl_4 solution could be observed in the IR spectra of reaction mixtures, recorded for several hours. When the experiment was conducted at 76 °C, however, the formation of isocyanate was clearly identified in the IR spectra (Figure 7A) with the appearance of a band with the typical frequency for the phenyl isocyanate N═C═O group at 2261 cm^{-1}. A gradual increase

dx.doi.org/10.1021/jo4002068 | J. Org. Chem. 2013, 78, 6440−6449

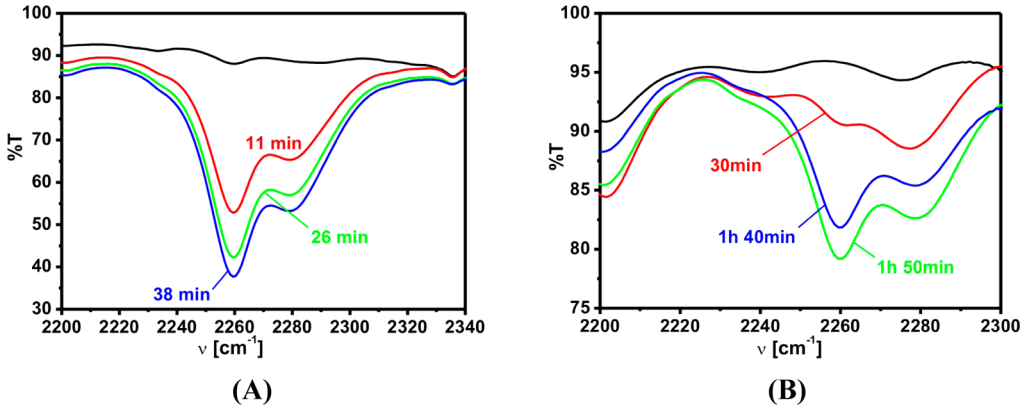

Figure 8. Formation of phenyl isocyanate from phenyl *N*-phenylcarbamate and *N*-methylpyrrolidine (A) and trimethylamine (B) at 76 °C in CCl_4.

Scheme 2. Arylcarbamates Considered

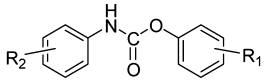

(1) R_2 =H; R_1 = H, 3-CH_3, 4-CH_3, 4-OCH_3, 3-Cl, 4-Cl, 4-Br, 3-NO_2, 4-NO_2

(2) R_1 =H; R_2 = H, 4-OCH_3, 4-Cl, 4-NO_2

(3) R_1=4-CH_3, R_2=4-Cl; R_1=4-Cl, R_2=3-CH_3; R_1=3-Cl, R_2=4-Cl;
R_1=4-CH_3, R_2=3-Cl; R_1=4-Cl, R_2=4-Cl; R_1=3-NO_2, R_2=4-CH_3;
R_1=4-Cl, R_2=4-CH_3; R_1=4-Cl, R_2=3-Cl; R_1=4-NO_2, R_2=4-CH_3

of the isocyanate concentration over several hours was observed. The accumulation of isocyanate is, evidently, a result of the much slower reverse reaction of PhNCO with the formed phenol to the initial phenyl *N*-phenylcarbamate. When the reaction mixture was left at room temperature for several hours, the intensity of the isocyanate band gradually decreased until disappearing (Figure 7B). Evidently, an equilibrium between phenyl *N*-phenylcarbamate and phenyl isocyanate is the reason for these temperature-dependent shifts. The important conclusion from these experiments is that an amine with basicity similar to that of *n*-butylamine and diethylamine is able to transform the carbamate into a stable isocyanate as result of a hydrogen extraction process. It may, therefore, be expected that *n*-butylamine and diethylamine should also be able to extract hydrogen from the carbamate and produce isocyanate in the principal reaction studied. The elimination of hydrogen from the −NH−CO−O− grouping may be considered as an example of an acid−base interaction and, thus, be governed mostly by the basic properties of the amine.

In general, however, the nucleophilicity of the amines may also affect the mechanism of the aminolysis. As shown for the hydrolysis reaction,[24] a shift of mechanistic routes may take place, depending on the leaving group and aryl substituents. It may be argued that amines possessing higher nucleophilicity will more readily attack the carbonyl group of the carbamate, thus favoring the $B_{AC}2$ route. The three amines considered so far (*n*-butylamine, diethylamine, and triethylamine) possess quite similar basicities, as discussed earlier. However, their nucleophilic parameters (Mayr nucleophilcity values, *N*)[43] differ in the following order: *n*-butylamine, 15.27; diethylamine, 15.10; triethylamine, 17.10.

To gain further insights into the effect of amine nucleophilicity vs basicity, we followed by IR spectroscopy the interaction between *N*-methylpyrrolidine and trimethylamine with phenyl *N*-phenylcarbamate. *N*-Methylpyrrolidine possesses distinctly higher nucleophilicity (N = 20.59)[43] but lower basicity (pK_a = 10.32)[42] in comparison to the other amines considered so far. In spite of its much higher nucleophilicity and lower basicity, *N*-methylpyrrolidine is also able to abstract a proton from the carbamate group, resulting in the formation of phenyl isocyanate. The N═C═O band appears at 2259 cm^{-1} on heating the reaction mixture at 76 °C (Figure 8A). We also conducted an analogous experiment with trimethylamine (a solution of Me_3N in tetrahydrofuran was used). Trimethylamine possesses distinctly lower basicity (pK_a = 9.80)[42] but high nucleophilicity (N = 23.05).[43] Thus, it offers good opportunities to test the influence of these properties on the aminolysis. The experiment was conducted in an open flask under reflux, containing phenyl *N*-phenylcarbamate dissolved in a 1:1 mixture of carbon tetrachloride and a tetrahydrofuran solution of Me_3N. The concentration of trimethylamine varied with time because of the low boiling temperature and evaporation. Nevertheless, the formation of a N═C═O band in the IR spectra (at 2260 cm^{-1}) was clearly identified, in spite of the complexity of the solvents and reactants (Figure 8B). It is seen that, despite its low basicity, trimethylamine is also able to abstract hydrogen from the −NH−CO−O− moiety and transform the carbamate into isocyanate under the conditions studied. The nucleophilicity of the amine does not appear to be of key importance for this hydrogen elimination process.

The proposed mechanism for the aminolysis of phenyl *N*-phenylcarbamate should not be automatically extrapolated to other carbamate aminolysis processes, since as shown[24] for the alkaline hydrolysis of carbamates, the mechanistic features depend strongly on the structures of all reactants.

Reactivity of Substituted Phenyl *N*-Phenylcarbamates in the Aminolysis Reaction. The reactivities of substituted phenyl *N*-phenylcarbamates in the aminolysis reaction were

dx.doi.org/10.1021/jo4002068 | J. Org. Chem. 2013, 78, 6440−6449

Table 3. Rate Constants and Reactivity Indexes for the Series of Substituted Phenyl *N*-Phenylcarbamates (Scheme 2)[a]

			Hirshfeld charge (e)		NBO charge (e)		EPN (V)		
R_1	R_2	log k_3[b]	q_N	q_H	q_N	q_H	ΔV_O[c]	ΔV_H[c]	σ^-
H	H	−4.60	−0.08128	0.13445	−0.63998	0.41056	0	0	0
3-CH_3	H	−4.78	−0.08151	0.13426	−0.64016	0.41044	−0.04607	−0.03358	−0.07
4-CH_3	H	−5.12	−0.08173	0.13401	−0.64042	0.41024	−0.06375	−0.04944	−0.17
4-OCH_3	H	−5.34	−0.08196	0.13391	−0.64082	0.41017	−0.09066	−0.06394	−0.26
3-Cl	H	−3.09	−0.07986	0.13552	−0.63823	0.41156	0.22576	0.14304	0.37
4-Cl	H	−3.67	−0.08022	0.13514	−0.63849	0.41118	0.20628	0.13910	0.19
4-Br	H	−3.55	−0.08005	0.13532	−0.63822	0.41131	0.23210	0.15466	0.25
3-NO_2	H	−1.76	−0.07796	0.13714	−0.63591	0.41294	0.49867	0.33781	0.71
4-NO_2	H	−1.18	−0.07787	0.13679	−0.63542	0.41264	0.57927	0.39280	1.27
r with log k_3			*0.995*	*0.984*	*0.995*	*0.984*	*0.993*	*0.992*	*0.976*
			Hirshfeld charge (e)		NBO charge (e)		EPN (V)		
R_1	R_2	log k_3[b]	q_N	q_H	q_N	q_H	ΔV_N[d]	ΔV_H[d]	σ^-
H	H	−4.60	−0.08128	0.13445	−0.63998	0.41056	0	0	0
H	4-Cl	−4.13	−0.08107	0.13596	−0.64053	0.41177	0.23575	0.19401	0.19
H	4-NO_2	−3.28	−0.07700	0.13876	−0.64008	0.41420	0.62797	0.56172	1.27
H	4-OCH_3	−4.70	−0.08334	0.13373	−0.63873	0.40983	−0.05641	−0.08938	−0.26
r with log k_3			*0.955*	*0.997*	*0.513*	*0.996*	*0.9997*	*0.998*	*0.983*
			Hirshfeld charge (e)		NBO charge (e)		EPN (V)		
R_1	R_2	log k_3[b]	q_N	q_H	q_N	q_H	ΔV_O[c]	ΔV_H[c]	
4-CH_3	4-Cl	−4.56	−0.08155	0.13554	−0.64111	0.41145	0.04887	0.15806	
4-CH_3	3-Cl	−4.44	−0.08032	0.13658	−0.64093	0.41229	0.05643	0.17327	
4-Cl	4-CH_3	−3.96	−0.08082	0.13477	−0.63774	0.41078	0.13559	0.06519	
4-Cl	3-CH_3	−3.80	−0.08022	0.13462	−0.63787	0.41084	0.15836	0.09352	
4-Cl	4-Cl	−3.33	−0.08023	0.13660	−0.63954	0.41236	0.32178	0.33604	
4-Cl	3-Cl	−3.09	−0.07875	0.13763	−0.63876	0.41321	0.33057	0.36328	
3-Cl	4-Cl	−2.73	−0.07891	0.13714	−0.63833	0.41293	0.33865	0.34562	
3-NO_2	4-CH_3	−1.18	−0.07853	0.13668	−0.63499	0.41247	0.43952	0.26693	
4-NO_2	4-CH_3	−1.16	−0.07847	0.13637	−0.63457	0.41218	0.53982	0.33542	

[a]The computations were performed at the M06-2X/6-311+G(2d,2p) level. [b]From ref 2. [c]ΔV_O refers to the C−O ester oxygen; $\Delta V_O = V_O(R) - V_O(H)$; $\Delta V_H = V_H(R) - V_H(H)$. $V_O(H)$ and $V_H(H)$ are the EPN values at the C−O oxygen and N−H hydrogen nuclei in the unsubstituted derivative. [d]$\Delta V_N = V_N(R) - V_N(H)$; $\Delta V_H = V_H(R) - V_H(H)$. $V_H(H)$ is the EPN value at the N−H hydrogen nucleus in the unsubstituted derivative.

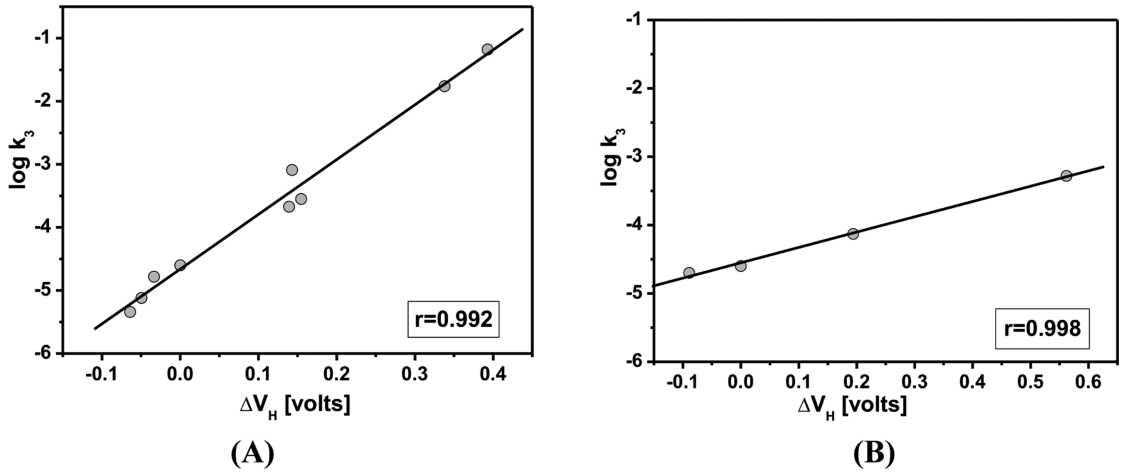

Figure 9. Plots of third-order experimental rate constants log k_3 (taken from ref 2) for the aminolysis of substituted phenyl *N*-phenylcarbamates with EPN values for the NH hydrogen atoms [$\Delta V_H = V_H(R) - V_H(H)$]: (A) series 1 and (B) series 2 from Scheme 2.

rationalized with the aid of electronic parameters. The three series of compounds examined are presented in Scheme 2.

The kinetic constants for the process, reported by Shawali et al.,[2] were employed in analyzing the relationships between structural variations and reactivity. We examined the effects of structural changes on several theoretical quantities that characterize the properties of particular atomic sites of the functional group involved in the aminolysis process. Three types of local reactivity descriptors were evaluated: NBO atomic charges,[37] Hirshfeld atomic charges,[38] and electrostatic potentials at the atoms[35,36] of the N−H group (V_N, V_H) in the reactant carbamates. As already discussed, the rate-controlling

dx.doi.org/10.1021/jo4002068 | J. Org. Chem. 2013, 78, 6440−6449

stage of the reaction under general base catalysis along the energetically favored E1cB pathway involves an attack of the amine nucleophile at the N−H group, resulting in the extraction of a hydrogen and formation of isocyanate.

The calculated reactivity indexes for the first series of aryl *N*-phenylcarbamates and the kinetic data employed[2] are summarized in Table 3. The final column in Table 3 contains the σ^- constants of the respective substituents. As discussed in the preceding section, the theoretical computations as well as the supporting experiments revealed that the general base-catalyzed aminolysis via isocyanate is the favored pathway for the reaction. Two main factors can be considered in regarding the possibility for the isocyanate mechanism for the aminolysis of arylcarbamates with a given amine as nucleophile: (1) the stability of the leaving group and (2) the acidity of the NH hydrogen atom in the reactant carbamate. We thus followed the influence of polar groups in the aromatic ring on the EPN values and NBO and Hirshfeld atomic charges of the N−H reaction center in the initial carbamate reactants. As expected, electron-withdrawing substituents increase the leaving group ability and favor the interaction between the two reactants. Inversely, electron-donating substituents, such as CH_3 and OCH_3, hamper the interaction with the nucleophile. Since hydrogen extraction was shown to be the rate-controlling stage of the reaction, the best correlations are obtained with theoretical parameters associated with the N−H hydrogen (correlation coefficients are given in Table 3).

The plot between the experimental third-order rate constant log k_3 values and the electronic index EPN is illustrated in Figure 9A. The results obtained demonstrate the accuracy of the theoretical description of the local properties of reactants.

The second series of compounds (Scheme 2), presented in the work of Shawali et al.,[2] consists of diarylcarbamates containing substituents in the aromatic ring next to the N−H bond, thus influencing the acidity of the N−H hydrogen atom. The electronic indexes considered reflect the influence of the substituents. Therefore, a correlation between these indexes and rate constants is expected as long as the first step of the reaction is rate determining. This consideration is valid, since the leaving groups are identical for all compounds in the series. A good correlation is obtained between the rate constants and electronic structure indexes, although the series contains only four compounds. These data are presented in Table 3, Figure 8B, and Figure S3 (Supporting Information). The third series in ref 2 includes diarylcarbamates with substituents in the phenyl rings at both amide and ester moieties of the carbamates. For these compounds the substituents play competitive roles in both factors: the stability of the leaving group and the acidity of the NH hydrogen atom. In this case, the intrinsic competition between two different factors, influencing the reaction rate, is not well reflected into a single electronic parameter. A correlation with two electronic parameters is established for all three series of molecules (eq 2).

$$\log k_3 = 1.37[\mathrm{EPN(O)}] - 0.47[\mathrm{EPN(H)}] + 0.02$$
$$n = 21 \quad r = 0.978 \qquad (2)$$

CONCLUDING REMARKS

Detailed theoretical modeling has been conducted for three possible reaction channels for both uncatalyzed and general base-catalyzed aminolysis of phenyl *N*-phenylcarbamate: concerted, stepwise addition−elimination via a tetrahedral intermediate ($B_{AC}2$), and a two-stage process involving intermediary formation of phenyl isocyanate (E1cB). The computational results reveal that the *isocyanate route is the most favorable pathway of the reaction*. The free energy barrier of the catalyzed E1cB process is 7.7 and 6.9 kcal/mol lower than the activation barriers of the concerted and $B_{AC}2$ mechanisms. The theoretical results were confirmed by an IR spectroscopic study on the reaction of phenyl *N*-phenylcarbamate with three amines with similar basicity: *n*-butylamine, diethylamine, and triethylamine. Two other tertiary amines, *N*-methylpyrrolidine and trimethylamine, with distinctly different basicities and nucleophilicities in comparison to the other amines considered, were also tested to assess the influence of amine properties on the processes investigated. The formation of the N═C═O band in the spectra is clearly manifested during the interaction of the carbamate with triethylamine and *N*-methylpyrrolidine, thus proving that isocyanate does indeed form under the attack of a nucleophile. In spite of its low basicity, trimethylamine also induces the formation of isocyanate under similar conditions. The amine basicity rather than nucleophilicity is considered to dominate the process of hydrogen abstraction and formation of isocyanate. The Ph−N═C═O intermediate is not directly observed during the reactions of phenyl *N*-phenylcarbamate with *n*-butylamine and diethylamine. The ready explanation for this finding is the high reactivity of the isocyanate in the interaction with these amines. Thus, fast consumption of the formed isocyanate does not allow its accumulation and detection in the infrared spectra. The reactivity of substituted phenyl *N*-phenylcarbamates is quantified by applying theoretically derived reactivity indexes (atomic charges and electrostatic potentials at nuclei values) for the atoms of the reaction center.

ASSOCIATED CONTENT

Supporting Information

Tables and figures giving comprehensive theoretical data, additional experimental data, and Cartesian coordinates and energies for all optimized structures along the reaction pathways studied. This material is available free of charge via the Internet at http://pubs.acs.org.

AUTHOR INFORMATION

Corresponding Author

*E-mail: silieva@chem.uni-sofia.bg; galabov@chem.uni-sofia.bg.

Notes

The authors declare no competing financial interest.

ACKNOWLEDGMENTS

This research was supported by FP7-REGPOT-2011-1 project BeyondEverest and BG051PO001/3.3-05 project Science and Business. We thank the reviewers for helpful suggestions.

REFERENCES

(1) Menger, F. M.; Glass, L. E. *J. Org. Chem.* **1974**, *39*, 2469−2470.
(2) Shawali, A. S.; Harhash, A.; Sidky, M. M.; Hassaneen, H. M.; Elkaabi, S. S. *J. Org. Chem.* **1986**, *51*, 3498−3501.
(3) Koh, H. K.; Kim, O. S.; Lee, H. W.; Lee, I. *J. Phys. Org. Chem.* **1997**, *10*, 725−730.
(4) Oh, H. K.; Park, J.; Sung, D. D.; Lee, I. *J. Org. Chem.* **2004**, *69*, 3150−3153.

(5) Oh, H. K.; Jin, Y.; Sung, D. D.; Lee, I. *Org. Biomol. Chem.* **2005**, *3*, 1240−1244.
(6) Castro, E. A.; Cubillos, M.; Iglesias, R.; Santos, J. G. *Int. J. Chem. Kinet.* **2012**, *44*, 604−611.
(7) Sung, K.; Zhuang, B.-R.; Huang, P.-M.; Jhong, S. W. *J. Org. Chem.* **2008**, *73*, 4027−4033.
(8) Lee, H. W.; Oh, H. K. *Bull. Korean Chem. Soc.* **2010**, *31*, 475−478.
(9) Bunnett, J. F.; Davis, G. T. *J. Am. Chem. Soc.* **1960**, *82*, 665−674.
(10) Jencks, W. P.; Carriuolo, J. *J. Am. Chem. Soc.* **1960**, *82*, 675−681.
(11) Bruice, T. C.; Mayahi, M. F. *J. Am. Chem. Soc.* **1960**, *82*, 3067−3071.
(12) Williams, A. *Acc. Chem. Res.* **1989**, *22*, 387−392.
(13) Castro, E. A. *Chem. Rev.* **1999**, *99*, 3505−3524.
(14) Oh, H. K.; Ku, M. H.; Lee, H. W.; Lee, I. *J. Org. Chem.* **2002**, *67*, 8995−8998.
(15) Singleton, D. A.; Merrigan, S. R. *J. Am. Chem. Soc.* **2000**, *122*, 11035−11036.
(16) (a) Um, I. H.; Min, J. S.; Ahn, J. A.; Hahn, H. J. *J. Org. Chem.* **2000**, *65*, 5659−5663. (b) Um, I. H.; Kim, K. H.; Park, H. R.; Fujio, M.; Tsuno, Y. *J. Org. Chem.* **2004**, *69*, 3937−3942.
(17) Ilieva, S.; Galabov, B.; Musaev, D.; Morokuma, K.; Schaefer, H. F., III *J. Org. Chem.* **2003**, *68*, 1496−1502.
(18) Galabov, B.; Atanasov, Y.; Ilieva, S.; Schaefer, H. F., III *J. Phys. Chem. A* **2005**, *109*, 11470−11474.
(19) Rangelov, M. A.; Vayssilov, G. N.; Yomtova, V. M.; Petkov, D. D. *J. Am. Chem. Soc.* **2006**, *128*, 4964−4965.
(20) Bruice, T. C.; Benkovic, S. J. *Bioorganic Mechanisms*; W. A. Benjamin: New York, 1966; Vol. *1*.
(21) Jencks, W. P. *Catalysis in Chemistry and Enzymology*; McGraw-Hill: New York, 1969.
(22) Page, M. I.; Williams, A. *Organic and Bioorganic Mechanisms*; Longmans: Harlow, U.K., 1997.
(23) (a) Ban, N.; Nissen, P.; Hanssen, J.; Moore, P. B.; Steitz, T. *Science* **2000**, *289*, 905−920. (b) Muth, G. W.; Ortoleva-Donnely, L.; Strobel, S. A. *Science* **2000**, *289*, 947−950.
(24) (a) Dittert, L. W.; Higuchi, T. *J. Pharm. Sci.* **1963**, *52*, 852−857. (b) Adams, P.; Baron, F. A. *Chem. Rev.* **1965**, *65*, 567−602. (c) Williams, A. *J. Chem. Soc., Perkin Trans. 2* **1972**, 808−812. (d) Hegarty, A. F.; Frost, L. N. *J. Chem. Soc., Perkin Trans. 2* **1973**, 1719−1728. (e) Bergon, M.; Calmon, J.- P. *Tetrahedron Lett.* **1981**, *22*, 937−940. (f) Wentworth, P., Jr.; Datta, A.; Smith, S.; Marshall, A.; Partridge, L. J.; Blackburn, G. M. *J. Am. Chem. Soc.* **1997**, *119*, 2315−2316.
(25) Furuya, Y.; Goto, S.; Itoho, K.; Urasaki, I.; Morita, A. *Tetrahedron* **1968**, *24*, 2367−2375.
(26) Furuya, Y.; Itoho, S. K.; Shibata, O.; Ohkubo, K. *Chem. Lett.* **1972**, *1*, 971−974.
(27) Frisch, M. J.; Trucks, G. W.; Schlegel, H. B.; Scuseria, G. E.; Robb, M. A.; Cheeseman, J. R.; Montgomery, J. A.; Vreven, T.; Kudin, K. N.; Burant, J. C.; Millam, J. M.; Iyengar, S. S.; Tomasi, J.; Barone, V.; Mennucci, B.; Cossi, M.; Scalmani, G.; Rega, N.; Petersson, G. A.; Nakatsuji, H.; Hada, M.; Ehara, M.; Toyota, K.; Fukuda, R.; Hasegawa, J.; Ishida, M.; Nakajima, T.; Honda, Y.; Kitao, O.; Nakai, H.; Klene, M.; Li, X.; Knox, J. E.; Hratchian, H. P.; Cross, J. B.; Bakken, V.; Adamo, C.; Jaramillo, J.; Gomperts, R.; Stratmann, R. E.; Yazyev, O.; Austin, A. J.; Cammi, R.; Pomelli, C.; Ochterski, J. W.; Ayala, P. Y.; Morokuma, K.; Voth, G. A.; Salvador, P.; Dannenberg, J. J.; Zakrzewski, V. G.; Dapprich, S.; Daniels, A. D.; Strain, M. C.; Farkas, O.; Malick, D. K.; Rabuck, A. D.; Raghavachari, K.; Foresman, J. B.; Ortiz, J. V.; Cui, Q.; Baboul, A. G.; Clifford, S.; Cioslowski, J.; Stefanov, B. B.; Liu, G.; Liashenko, A.; Piskorz, P.; Komaromi, I.; Martin, R. L.; Fox, D. J.; Keith, T.; Al-Laham, M. A.; Peng, C. Y.; Nanayakkara, A.; Challacombe, M.; Gill, P. M. W.; Johnson, B.; Chen, W.; Wong, M. W.; Gonzalez, C.; Pople, J. A. *Gaussian 09 (Revision-A.01)*; Gaussian, Inc., Wallingford, CT, 2009.
(28) (a) Becke, A. D. *J. Chem. Phys.* **1993**, *98*, 5648−5652. (b) Becke, A. D. *J. Chem. Phys.* **1996**, *104*, 1040−1046. (c) Lee, C. T.; Yang, W. T.; Parr, R. G. *Phys. Rev. B* **1988**, *37*, 785−789.
(29) (a) Zhao, Y.; Truhlar, D. G. *Theor. Chem. Acc.* **2008**, *120*, 215−241. (b) Zhao, Y.; Truhlar, D. G. *J. Chem. Theory Comput.* **2008**, *4*, 1849−1868.
(30) (a) Curtiss, L. A.; McGrath, M. P.; Blaudeau, J. P.; Davis, N. E.; Binning, R. C., Jr.; Radom, L. *J. Chem. Phys.* **1995**, *103*, 6104−6113. (b) Clark, T.; Chandrasekar, G. W., J.; Schleyer, P. v. R. *J. Comput. Chem.* **1983**, *4*, 294−301.
(31) Grimme, S.; Antony, J.; Ehrlich, S.; Krieg, H. *J. Chem. Phys.* **2010**, *132*, 154104−154122.
(32) Goerigk, L.; Grimme, S. *J. Chem. Theory Comput.* **2010**, *6*, 107−126.
(33) Gonzalez, C.; Schlegel, H. B. *J. Chem. Phys.* **1989**, *90*, 2154−2161.
(34) Tomasi, J.; Mennucci, B.; Cammi, R. *Chem. Rev.* **2005**, *105*, 2999−3093.
(35) Wilson, E. B. *J. Chem. Phys.* **1962**, *36*, 2232−2233.
(36) Politzer, P. In *Chemical Applications of Atomic and Molecular Electrostatic Potentials*; Politzer, P., Truhlar, D. G., Eds.; Plenum Press: New York, 1981; p 7.
(37) (a) Reed, A. E.; Weinstock, R. B.; Weinhold, F. *J. Chem. Phys.* **1985**, *83*, 735−746. (b) Reed, A. E.; Curtiss, L. A.; Weinhold, F. *Chem. Rev.* **1988**, *88*, 899−926.
(38) (a) Hirshfeld, F. L. *Theor. Chem. Acc.* **1977**, *44*, 129−138. (b) Ritchie, J. P. *J. Am. Chem. Soc.* **1985**, *107*, 1829−1837. (c) Ritchie, J. P.; Bachrach, S. M. *J. Comput. Chem.* **1987**, *8*, 499−509.
(39) Hammett, L. P. *J. Am. Chem. Soc.* **1937**, *59*, 96−103.
(40) Hansch, C.; Leo, A.; Taft, W. *Chem. Rev.* **1991**, *91*, 165−195.
(41) Ivanova, E. V.; Muchall, H. D. *J. Phys. Chem.* **2007**, *111*, 10824−10833.
(42) (a) Perrin, D. D., *Dissociation Constants of Organic Bases in Aqueous Solution*; Butterworths: London, 1965 (Supplement, 1972). (b) Serjeant, E. P.; Dempsey, B., *Ionization Constants of Organic Acids in Aqueous Solution*; Pergamon: Oxford, U.K., 1979.
(43) (a) Kanzian, T.; Nigst, T. A.; Maier, A.; Pichl, S.; Mayr, H. *Eur. J. Org. Chem.* **2009**, 6379−6385. (b) Ammer, J.; Baidya, M.; Kobayashi, S.; Mayr, H. *J. Phys. Org. Chem.* **2010**, *23*, 1029−1035. (c) Nigst, T. A.; Antipova, A.; Mayr, H. *J. Org. Chem.* **2012**, *77*, 8142−8155.